Quaternary half-metallic Heusler ferromagnets for spintronics applications

Vajiheh Alijani, Juergen Winterlik, Gerhard H. Fecher, S. Shahab Naghavi, and Claudia Felser*
Institut für Anorganische und Analytische Chemie, Johannes Gutenberg–Universität, D-55099 Mainz, Germany
(Received 20 January 2011; revised manuscript received 21 March 2011; published 25 May 2011)

This work reports on three quaternary Heusler compounds NiFeMnGa, NiCoMnGa, and CuCoMnGa. In contrast to their ternary relatives, quaternary Heusler compounds are still rarely investigated. A very large pool of interesting materials lies thus idle waiting for exploration. The difficulty consists in choosing prospective compositions, and *trial and error* is elaborate and expensive. We have identified several candidates employing *ab initio* electronic-structure calculations. The compounds were synthesized, and the structural and magnetic properties were investigated experimentally. CuCoMnGa is a quaternary Heusler compound; NiFeMnGa and NiCoMnGa are unreported half-metallic ferromagnetic materials with potential for spintronics applications.

DOI: 10.1103/PhysRevB.83.184428 PACS number(s): 81.05.Zx, 85.75.−d, 75.20.En, 73.22.Pr

I. INTRODUCTION

The $T_2T'M$ (T,T' = transition metals, M = main group element) Heusler compounds are ternary intermetallics with a 2 : 1 : 1 stoichiometry.[1,2] They attracted the interest of the magnetism community when Heusler *et al.*[1,3] showed that the compound Cu_2MnAl becomes ferromagnetic, even though none of its constituents is ferromagnetic by itself. Interest in the Heusler compounds has increased since it was established that their properties can easily be altered by substitution of elements. Co_2-based compounds were already synthesized and investigated in the 1960s and 1970s.[4,5] Later the predicted half-metallic ferromagnets came into the center of attention.[6,7] Today Heusler compounds are used for various applications in the research fields of spintronics,[8] thermoelectrics,[9,10] and superconductors.[11] Yet quaternary half-metallic Heusler compounds are very rarely investigated. A multitude of compounds of this class with interesting properties can thus be uncovered using appropriate tools for exploration. We have used *ab initio* electronic-structure calculations to identify interesting half-metallic compounds for spintronics applications. In the current work we present the results of theoretical, structural, and magnetic investigations of the unreported half-metallic quaternary Heusler ferromagnets NiFeMnGa and NiCoMnGa. To the best of our knowledge, these are actually the first Ni-based half-metallic ferromagnets reported up to now. We have also characterized the unreported quaternary Heusler compound CuCoMnGa. This compound is, however, of minor technological importance because the closed d shell of copper inhibits half-metallic ferromagnetism.

II. EXPERIMENTAL AND CALCULATIONAL DETAILS

Polycrystalline ingots of NiFeMnGa, NiCoMnGa, and CuCoMnGa were prepared by repeated arc melting of stoichiometric mixtures of high-purity elements in an argon atmosphere. Care was taken to minimize contamination by O_2. Therefore, a titanium sponge was employed as an oxygen getter before the samples were melted. The samples were melted four times and turned in between to ensure homogeneity. The resulting ingots were annealed in evacuated quartz tubes for 14 days at 800 °C. The crystal structure was investigated by x-ray powder diffraction (XRD) equipped with an x-ray tube using Mo $K\alpha$ radiation (Bruker D8 Advance). The magnetic properties of the polycrystalline samples were investigated by a superconducting quantum interference device (SQUID, Quantum Design MPMS-XL-5) using small pieces of approximately 30–40 mg.

The electronic structures of the compounds were calculated by means of the full-potential linearized augmented-plane-wave (FLAPW) method as implemented in WIEN2k provided by Blaha, Schwarz, and co-workers.[12–14] The exchange-correlation functional was taken within the generalized-gradient approximation (GGA) in the parametrization of Perdew, Burke, and Enzerhof (PBE).[15] A 25 × 25 × 25 point mesh was used as a base for the integration in the cubic systems, resulting in 455 k points in the irreducible wedge of the Brillouin zone. The energy convergence criterion was set to 10^{-5} Ry and simultaneously the criterion for charge convergence to $10^{-3}e^-$. The number of plane waves was restricted by $Rk_{\max} = 7$. A convergence test for NiFeMnGa as well as many other Heusler compounds[16] revealed that this criterion is sufficient for systems with $L2_1$, X, Y, or $C1_b$ structure, due to the closed packing of these fcc-type structures. The muffin-tin radii were set to $2.5a_{0B}$ (a_{0B} represents Bohr's radius) for the transition metals as well as the main group elements.

Further electronic-structure calculations were carried out using the full relativistic spin-polarized Korringa-Kohn-Rostoker method (SPRKKR) provided by Ebert *et al.*[17–19] This program provides the coherent potential approximation (CPA) for calculating the properties of alloy systems with random distribution of the atoms. The SPRKKR calculations were performed using the PBE generalized gradient approximation.[15] The CPA tolerance was set to 10^{-4} and the energy convergence criterion to 10^{-5}. f states were included in the basis of all atoms. A total of 832 irreducible k points based on a 22 × 22 × 22 mesh were used for integration. The density of states is calculated for the double number of k points from the Green's function by adding a small imaginary part of 0.002 Ry to the energy. For smaller values, the band gaps may become better visible, however at the same time the density of states (DOS) becomes much more noisy.

III. RESULTS AND DISCUSSION

A. Electronic structure

The starting point for the electronic-structure calculations was an optimization of the cubic structure, i.e., a search of the

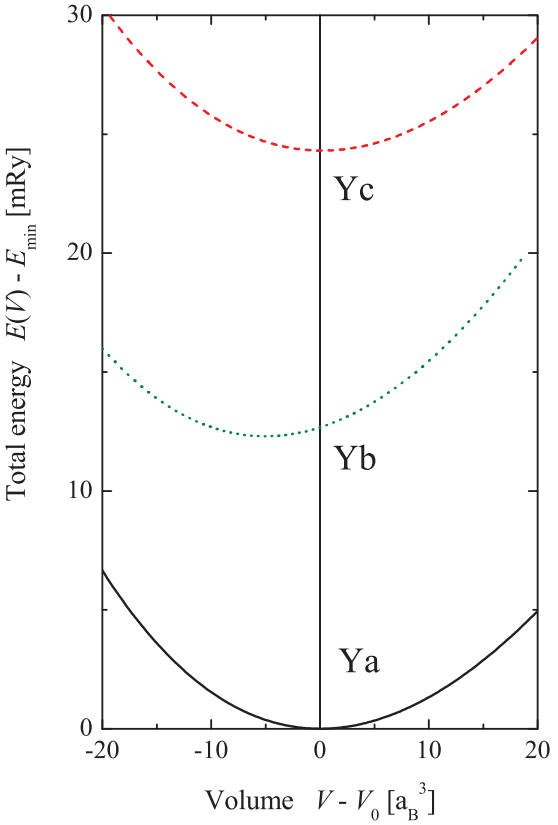

FIG. 1. (Color online) Structure dependence of the total energy of CuCoMnGa. Shown is the volume dependence of the total energy for the three possible different site occupations Ya: CuCoMnGa, Yb: CoMnCuGa, and Yc: CuMnCoGa.

minimum total energy as a function of the lattice parameter and site occupation. For all three compounds, the optimization of the cubic lattice parameter revealed the lowest energy for the structure with M on Wyckoff position 4a, T' on 4b, T on 4c, and T'' on 4d on the lattice with space group $F\bar{4}3m$ (see Sec. III B). Starting, for example, with opposite moments at the Mn and Co sites of CuCoMnGa, the calculations always converged into a state with parallel moments at Co and Mn, i.e., no ferrimagnetic ground state was observed for one of the three structures. The dependence of the total energy on the crystal structure and the lattice parameter is shown in Fig. 1.

TABLE I. Elastic constants of CoFeMnZ compounds. The optimized lattice parameter a_{calc} is given in angstroms; all values c_{ij} and the bulk modulus B are given in GPa. The elastic anisotropy $A_e = 2c_{44}/(c_{11} - c_{12})$ is dimensionless.

Compound	a_{calc}	c_{11}	c_{12}	c_{44}	B	A_e
NiFeMnGa	5.755	208	176	151	186	9.4
NiCoMnGa	5.784	186	172	119	177	17
CuCoMnGa	5.846	65	184	153	144	−2.6

Furthermore, the stability of the cubic structure was checked by calculation of the elastic constants c_{ij}. The three independent elastic constants of the cubic structure (c_{11}, c_{12}, and c_{44}) were calculated by applying isotropic strain as well as volume-conserving tetragonal and rhombohedral strains to the optimized primitive cubic cell.

The results of the calculated elastic properties are summarized in Table I. As a result of a negative tetragonal shear modulus ($c_{11} - c_{12}$), the elastic anisotropy of CuCoMnGa becomes also negative. This clearly points to a structural instability of CuCoMnGa, whereas the Ni-containing compounds turned out to be structurally stable.

Figure 2 shows the calculated band structure and density of states of NiFeMnGa. It is evident that the compound exhibits a half-metallic ferromagnetic band structure and the minority channel shows a gap at the Fermi energy. NiCoMnGa was also identified to exhibit a half-metallic ferromagnetic ground state. In contrast to these findings, CuCoMnGa has states at the Fermi energy in both spin directions and is thus a normal metal. Figure 3 shows the corresponding band structure and density of states for comparison. Table II summarizes the magnetic moments obtained from the electronic-structure calculations.

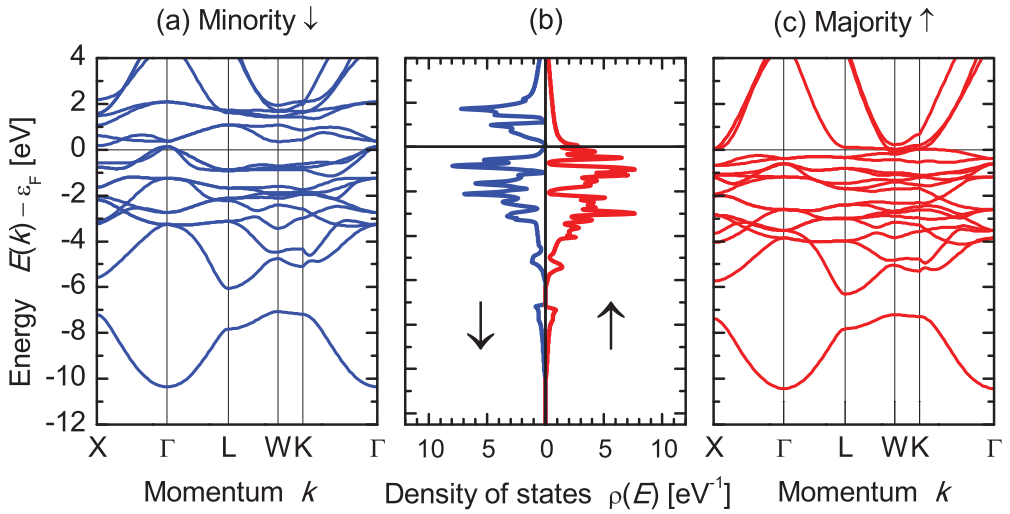

FIG. 2. (Color online) Band structure and density of states of NiFeMnGa. (a) Minority bands, (b) density of states, and (c) majority bands. Majority and minority spin densities are denoted by ↑ and ↓, respectively.

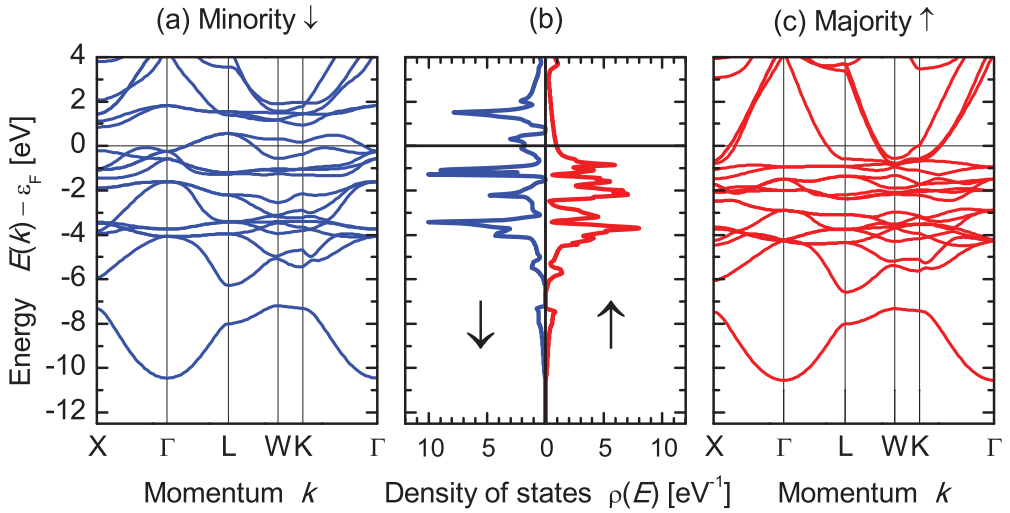

FIG. 3. (Color online) Band structure and density of states of CuCoMnGa. (a) Minority bands, (b) density of states, (c) and majority bands. Majority and minority spin densities are denoted by ↑ and ↓, respectively.

For CuCoMnGa, calculations were performed assuming different types of antisite disorder. Besides the ordered Y-type structure, the $A2$ ($I\,m\bar{3}m$, W-type), $B2$ ($P\,m\bar{3}m$, CsCl-type), and a disordered $L2_1$ ($F\,m\bar{3}m$, Cu_2MnAl-type) variation were assumed (see also Ref. 20). In $A2$, all sites are randomly occupied by one-quarter of the different atom types. For $B2$ it was assumed that Co and Cu are distributed on one site of the CsCl cell and Mn and Ga on the second site. For the disordered $L2_1$ structure, Cu and Co randomly occupy the 8c Wyckoff position of the $F\,m\bar{3}m$ lattice, while Mn and Ga occupy the positions 4b and 4a, respectively. The KKR-CPA method was used to account for the random site occupation. The lattice parameter was set to $a = 5.846$ Å in all four cases.

Figure 4 compares the density of states of well-ordered Y-type CuCoMnAl to the three major disordered variations of the cubic structure: $L2_1$, $B2$, and $A2$. It is seen that the density of states becomes smeared out with an increasing degree of disorder. In the $B2$ and $A2$ structures, even the Heusler-typical hybridization gap (seen at about -6.6 eV for Y and $L2_1$), which separates the low-lying s bands from the higher-lying p and d bands, vanished. The Fermi energy is located in a minimum of the total density in the $L2_1$- and $B2$-type structures. This may stabilize or enhance these types of disorder in the compound. The Fermi energy is also trapped in or close to a minimum of the minority density of states. This behavior stabilizes the magnetic moments at approximately $4\mu_B$.

TABLE II. Calculated magnetic moments of NiFeMnGa, NiCoMnGa, and CuCoMnGa. All values are given in μ_B. Note that the Mn atoms in this structure correspond to T' and occupy the Wyckoff position 4b.

TT''MnGa	m_{tot}	m_T	$m_{T''}$	m_{Mn}
NiFeMnGa	4.01	0.47	0.79	2.84
NiCoMnGa	5.07	0.59	1.22	3.26
CuCoMnGa	4.32	0.08	0.97	3.27

Table III compares the magnetic moments in the disordered and ordered structures assumed for CuCoMnGa. The total

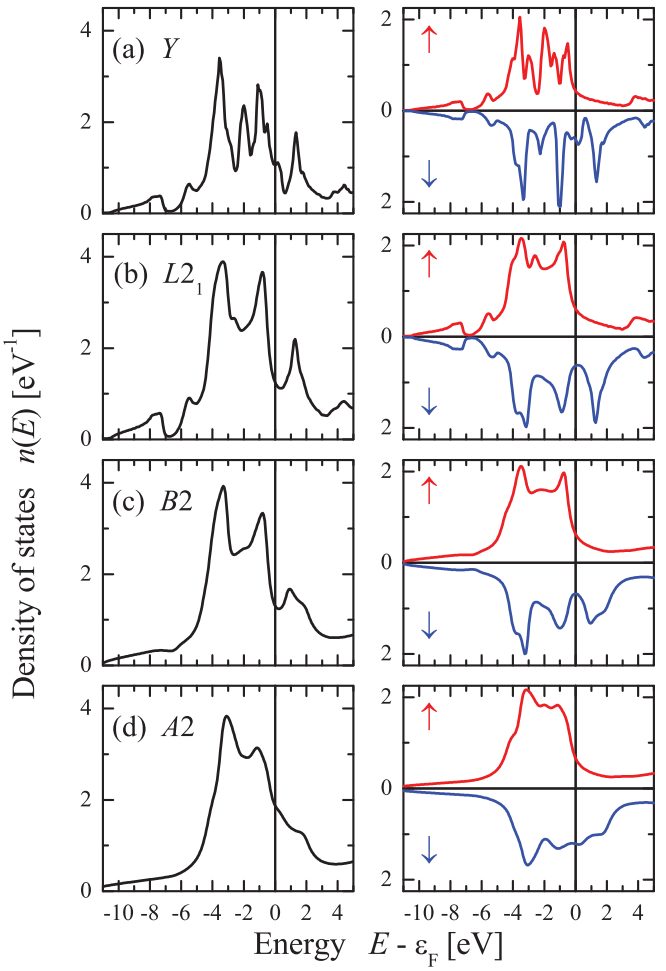

FIG. 4. (Color online) Electronic structure of disordered CuCoMnGa. Compared is the total and spin-resolved density of states for the ordered (a) compound and three possible types of disorder (b) $L2_1$, (c) $B2$, and (d) $A2$. Majority and minority densities are denoted by up and down arrows, respectively.

TABLE III. Calculated magnetic moments of disordered CuCoMnGa. All values are given in μ_B. Total spin moments of $A2$ and $B2$ are given for the primitive cell of the Y structure. Site-resolved moments are given per atom.

	Symmetry	m_{tot}	m_{Co}	m_{Mn}
$A2$	$I\,m\bar{3}m$	4.09	1.42	2.69
$B2$	$P\,m\bar{3}m$	4.17	0.91	3.26
$L2_1$	$F\,m\bar{3}m$	4.08	0.87	3.25
Y	$F\,\bar{4}3m$	3.98	0.7	3.28

spin magnetic moments stay, independent of the structure, at approximately $4\mu_B$ with respect to the fcc primitive cell with a basis of four atoms. The magnetic moment in the Y structure using SPRKKR is slightly smaller as in the FLAPW calculations, where the moment at the Co site was slightly higher. This is due to the neglect of the full symmetry potential in the SPRKKR method used here.

B. Structural characterization

Various types of ordered and disordered structures of Heusler compounds were discussed by Bacon and Plant.[20] The $L2_1$ structure of the ternary Heusler compounds with a 2 : 1 : 1 stoichiometry is a perfect 2^3 CsCl superstructure. The T_2 atoms form a primitive cubic sublattice, and adjacent cubes of this T_2 sublattice are filled alternating by T' or M atoms [see Fig. 5(a)]. The primitive cell of the $L2_1$ structure contains four atoms that form the base of the fcc primitive cell. The result is a lattice with $F\,m\bar{3}m$ symmetry where the Wyckoff positions 4a (0, 0, 0), 4b (1/2, 1/2, 1/2), and 8c (1/4,1/4, 1/4) are occupied by M, T', and T_2, respectively. The simple-cubic sublattice is lost if one of the T_2 atoms is replaced by a third type of transition metal T''. At the same time, the symmetry is lowered to $F\,\bar{4}3m$ (the center of inversion is removed in this symmetry). In this so-called Y structure, the Wyckoff positions 4a (0, 0, 0), 4b (1/2, 1/2, 1/2), 4c (1/4, 1/4, 1/4), and 4d (3/4, 3/4, 3/4) are occupied by M, T', T, and T'', respectively [see Fig. 5(c)]. The prototype of this structure is LiMgPdSn. Transforming the quaternary 1 : 1 : 1 : 1 compound back to a ternary but replacing T' by T does not change the $F\,\bar{4}3m$ symmetry [see Fig. 5(b)]. This transformation leads to the so-called X structure, which often appears for Heusler compounds when the ordinal number of the T' element is larger than that of the T element [$Z(T') > Z(T)$] and both elements are from the same period (i.e., $3d$ transition metals). It should be mentioned that all three structure types are converted into a simple bcc structure ($A2$, $I\,m\bar{3}m$) when all four positions are filled with identical atoms. This is the case for Heusler compounds in particular, with a random occupation of all lattice sites, i.e., complete disorder.

Figure 6 shows the powder diffraction data of the three compounds measured at room temperature. The diffraction data confirm the cubic LiPdMgSn crystal structures for all compounds. Note that the (111) and (200) fcc superstructure reflections are not resolved for all compounds due to nearly equal scattering amplitudes of the constituting elements, which are all found in the third period of the Periodic Table. A discussion of disorder phenomena as known from related Heusler compounds is therefore not possible. A deeper insight into the structure is a task for the future and could be achieved employing methods such as anomalous XRD or extended x-ray absorption fine structure (EXAFS). Rietveld refinements of the data were performed using the TOPAS ACADEMIC software package.[21] The lattice parameters as deduced from the refinements as well as the Rietveld figures of merit are shown in Table IV and compared to the calculated, structural data. The calculated bulk moduli of the Ni compounds are in the order of 180–190 GPa, whereas the Cu compound is obviously softer with an ≈30% lower value.

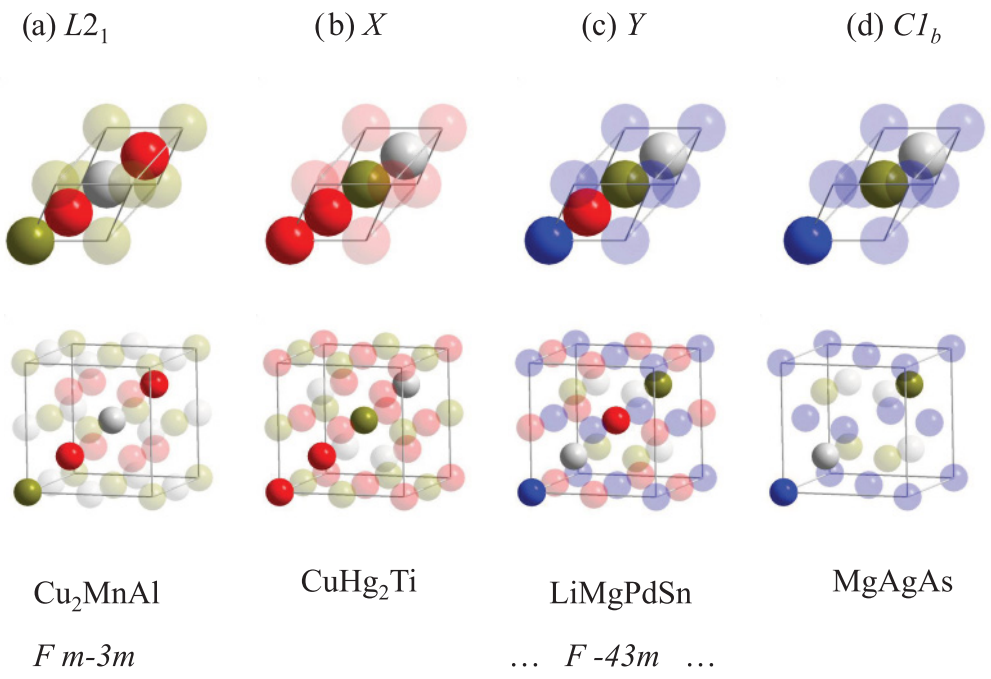

FIG. 5. (Color online) Different crystal structures of well-ordered Heusler compounds.

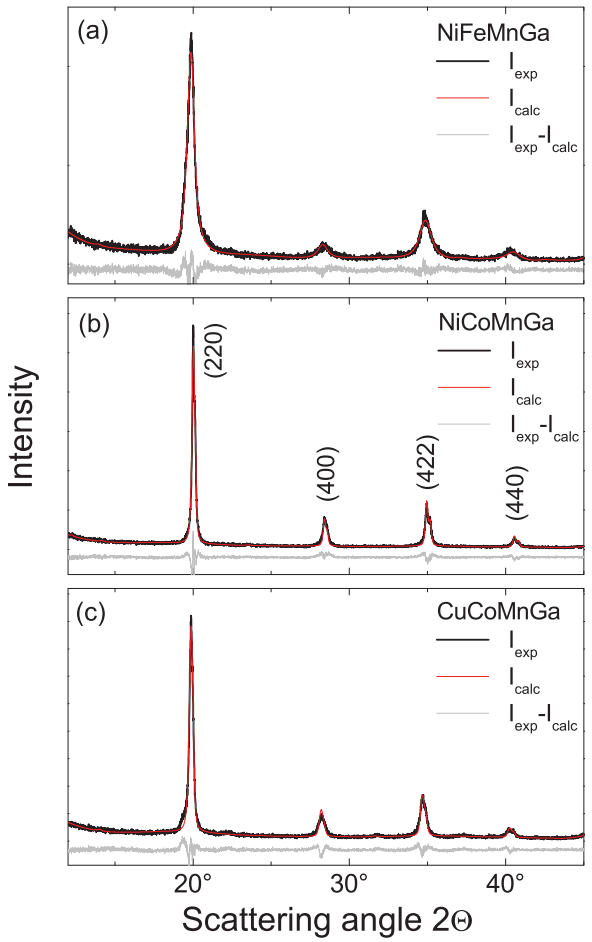

FIG. 6. (Color online) Powder XRD of polycrystalline NiFeMnGa, NiCoMnGa, and CuCoMnGa. The data were recorded at room temperature using Mo $K\alpha$ radiation.

C. Magnetic properties

The magnetic moments of Heusler compounds, especially Co_2-based half-metallic ferromagnets, follow the Slater-Pauling rule in which, for localized moment systems, an average magnetic moment per atom of

$$m_{\mathrm{av}} = (n_{\mathrm{av}} - 6 - 2n_{\mathrm{sp}})\mu_B \tag{1}$$

results. n_{av} is the mean number of valence electrons per atom in a compound, and n_{sp} arises from the average number of unbalanced minority sp electrons. The value 6 arises from the fact that the d electrons are constrained such that the Fermi energy falls into a minimum (or gap) between occupied and unoccupied d states and therefore minimizes the total energy. In half-metallic ferromagnets with a gap in one of the spin densities or in quasi-closed-shell compounds, all sp electrons are occupied, and the n_{sp} term vanishes. In 2 : 1 : 1 or 1 : 1 : 1 Heusler compounds, there are four atoms in the primitive cell and the total magnetic moment thus amounts to

$$m_{\mathrm{loc}} = (N_v - 24)\mu_B. \tag{2}$$

N_v is the accumulated number of valence electrons in the primitive cell (for details, see Refs. 16,22–24). The valence electron count means $2 + n(d)$ for each transition metal and $2 + n(p)$ for the main group elements, where 2 arises in both cases from the s electrons and $n(d)$ and $n(p)$ are the numbers of d and p valence electrons, respectively. At $N_v = 24$, the materials are not ferromagnetic according to the Slater-Pauling rule. The reason is that a quasi-closed-shell character is reached at a filling of the bands by 24 valence electrons. It is caused by successive filling of the a_1 (two s electrons), t_2 (six p electrons), e, and t_2 (ten d electrons) bands, followed by subsequent complete filling of an additional t_2 band (six d electrons). Deviations from Eq. (2) will appear when the compound is not in a half-metallic state, and unbalanced sp or d electrons are present. In certain cases of $L2_1$ ordered Heusler compounds, 24 valence electrons lead to the phenomenon of half-metallic completely compensated ferrimagnetism,[25] where the moments are ordered in a way that the total magnetic moment vanishes even though individual magnetic moments are of different magnitudes, in contrast to antiferromagnets.[26]

For high valence electron concentrations ($N_v \geqslant 30$), the assumption of localized behavior may no longer hold. Heusler compounds with moments much larger than $6\mu_B$ are rarely known. For higher valence electron concentrations, an itinerant Slater-Pauling behavior is approximated where the magnetic moment is determined by constraining the Fermi energy by the filled majority states.[22,24] The following approximation is valid for these certain cases of Heusler compounds:

$$m_{\mathrm{it}} \approx (34 - N_v)\mu_B. \tag{3}$$

This behavior is expected for d elements with nearly filled d shells as is the case for Ni (or Cu) and is obtained for various Ni_2-based Heusler compounds.[27] Here, the Cu-containing compound follows obviously this rule and the itinerant behavior may arise from the CuCo sublattice. Indeed, because of the localized moment at the Mn atoms, the behavior is not purely itinerant. The rule given by Eq. (3) hints that approximately 17 majority states are occupied[24,27] corresponding to T_d symmetry with a complete filling of one a_1, two e, and four t_2 majority bands.

The magnetic properties of the polycrystalline samples were investigated by means of SQUID magnetometry. The field-dependent magnetic moments at low temperature (5 K) are displayed in Fig. 7. The inset shows temperature-dependent measurements of the magnetizations. All compounds are soft-magnetic. The saturation magnetic moments of the compounds

TABLE IV. Lattice parameters and Rietveld figures of merit of the NiFeMnGa, NiCoMnGa, and CuCoMnGa compounds.

Compound	a_{exp}	R_{wp}	R_{exp}	R_{Bragg}	GoF
NiFeMnGa	5.799 Å	11.99%	8.27%	2.19%	1.45
NiCoMnGa	5.803 Å	11.63%	8.10%	2.48%	1.44
CuCoMnGa	5.847 Å	11.32%	8.63%	1.51%	1.31

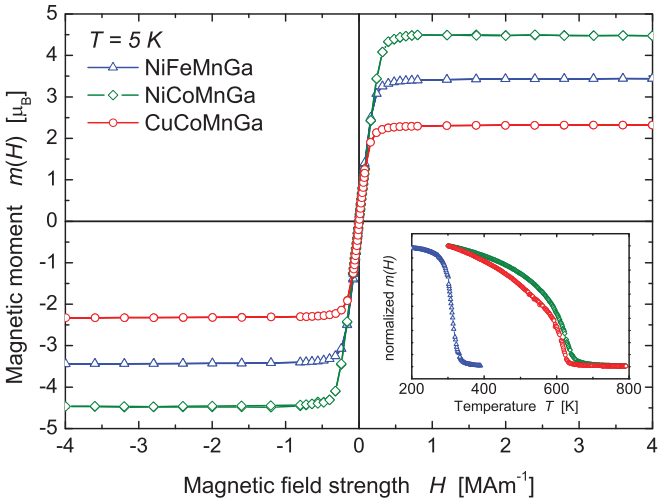

FIG. 7. (Color online) Magnetic properties of NiFeMnGa, NiCoMnGa, and CuCoMnGa. The MH-curves were measured at $T = 5$ K. The inset shows temperature dependent measurements of the magnetic moments in order to determine T_C.

are summarized in Table V. The calculated contributions of each atom in total magnetic moment are summarized in Table II. According to the Slater-Pauling rule and the electronic-structure calculations, the magnetic moment for NiFeMnGa should amount to $4\mu_B$ and for NiCoMnGa to $5\mu_B$. The discrepancy between these and the experimental values is quite large. It could be attributed to structural disorder, but the order of magnitude is too high to be dedicated only on this effect. Impurities below the detection limit of XRD (approximately 5%) may also contribute to the deviations. A ferrimagnetic arrangement or canted spins are possible but energetically unstable for all compounds according to the calculations. Antisite disorder may, however, lead to local ferrimagnetic order of the Mn atoms when they are nearest neighbors.

The magnetic moment of CuCoMnGa with $N_v = 30$ should amount to $6\mu_B$ when assuming half-metallicity and a localized Slater-Pauling behavior [Eq. (2)], which is in disagreement with the calculational and the experimental results. However, for an itinerant Slater-Pauling behavior [Eq. (3)], the expected moment is only $4\mu_B$. The lower magnetic moment is explained by the vanishing contribution of Cu to the magnetic properties due to the filled d shell, which makes a localized Slater-Pauling behavior—in the form presented in Eq. (2)—impossible. Although the calculation did not result in a half-metallic ferromagnetic state, the experimental value is also still too small compared to the calculation for a simple, regular ferromagnet. The low magnetic moment may also be a result of disorder and/or undetected impurities below the limit of powder XRD. The occurrence of disorder may be explained by the structural instability suggested by the calculations. As

TABLE V. Magnetic moments of the compounds at 5 and 300 K and Curie temperatures T_C.

Compound	$m_{\text{exp}}(5\text{ K})$ (μ_B)	$m_{\text{exp}}(300\text{ K})$ (μ_B)	T_C (K)
NiFeMnGa	3.45	1.74	326
NiCoMnGa	4.47	4.28	646
CuCoMnGa	2.32	2.14	631

for the other two compounds, antisite disorder may lead to local ferrimagnetic order of next-neighbor Mn atoms with the result of a lower total magnetic moment. This effect is not accounted for in the CPA calculations.

NiFeMnGa and NiCoMnGa, however, show at least fair agreement with the Slater-Pauling rule and thus half-metallic ferromagnetic behavior, which makes the compounds attractive for the research area of spintronics. The high T_C of NiCoMnGa makes the compound even more attractive for application. Optimizing annealing temperatures and times could provide help to obtain a better quality of the samples with respect to disorder and impurities. While NiCoMnGa and CuCoMnGa show a textbook ferromagnetic behavior, NiFeMnGa exhibits a rather sharp drop of magnetization at T_C. This may be due to a structural transformation and remains to be analyzed in future experiments (high-temperature XRD).

IV. SUMMARY

In conclusion, we have identified quaternary Heusler compounds using a theoretical approach for preselection. As predicted by these calculations, we have found the half-metallic ferromagnets NiFeMnGa and NiCoMnGa. To the best of our knowledge, these are the first reported Ni-based half-metallic ferromagnets within the huge family of Heusler compounds. CuCoMnGa turned out to be a regular metallic ferromagnet due to the closed-shell character of the Cu d electrons. NiFeMnGa has a Curie temperature that is too low to make it relevant for technological applications, but NiCoMnGa, which has a high spin polarization, high magnetic moment, and Curie temperature, is an interesting new material for spintronics applications. A large resource of quaternary Heusler materials is available to be investigated in the future to find prospective materials for several applications.

ACKNOWLEDGMENTS

This work was financially supported by the Deutsche Forschungsgemeinschaft DfG (projects TP 1.2-A and TP 2.3-A of research unit FOR 1464 Advanced spintronic materials and transport phenomena *ASPIMATT*). S.H. acknowledges the support of the graduate school of excellence MAINZ-MATCOR.

*felser@uni-mainz.de

[1] F. Heusler, Verh. Dtsch. Phys. Ges. **5**, 219 (1903).
[2] O. Heusler, Ann. Phys. **411**, 155 (1934).
[3] F. Heusler, W. Starck, and E. Haupt, Verh. Dtsch. Phys. Ges. **5**, 220 (1903).
[4] V. Y. Markiv, E. I. Hladyshevskii, and Y. B. Kuzma, Dop. Akad. Nauk Ukr. RSR, 1329 (1962).
[5] P. J. Webster, J. Phys. Chem. Solids **32**, 1221 (1971).
[6] J. Kübler, A. R. Williams, and C. B. Sommers, Phys. Rev. B **28**, 1745 (1983).

[7]R. A. de Groot, F. M. Mueller, P. G. van Engen, and K. H. J. Buschow, Phys. Rev. Lett. **50**, 2024 (1983).
[8]C. Felser, G. H. Fecher, and B. Balke, Angew. Chem. Int. Ed. **46**, 668 (2007).
[9]N. Shutoh and S. Sakurada, J. Alloys Compd. **289**, 204 (2005).
[10]C. S. Lue and Y.-K. Kuo, Phys. Rev. B **66**, 085121 (2002).
[11]J. Winterlik, G. H. Fecher, and C. Felser, Solid State Commun. **145**, 475 (2008).
[12]P. Blaha, K. Schwarz, P. Sorantin, and S. B. Tricky, Comput. Phys. Commun. **59**, 399 (1990).
[13]P. Blaha, K. Schwarz, G. K. H. Madsen, D. Kvasnicka, and J. Luitz, *WIEN2k, An Augmented Plane Wave + Local Orbitals Program for Calculating Crystal Properties* (Karlheinz Schwarz, Techn. Universitaet Wien, Wien, Austria, 2001).
[14]K. Schwarz, P. Blaha, and G. K. H. Madsen, Comput. Phys. Commun. **147**, 71 (2002).
[15]J. P. Perdew, K. Burke, and M. Ernzerhof, Phys. Rev. Lett. **77**, 3865 (1996).
[16]H. C. Kandpal, G. H. Fecher, and C. Felser, J. Phys. D **40**, 1507 (2007).
[17]H. Ebert, in *Electronic Structure and Physical Properties of Solids, The Use of the LMTO Method*, Lecture Notes in Physics Vol. 535, edited by H. Dreysee (Springer-Verlag, Berlin, 1999), p. 191.
[18]H. Ebert, *The Munich SPR-KKR package, Version 3.6*, [http://olymp.cup.uni-muenchen.de/ak/ebert/SPRKKR] (2005).
[19]H. Ebert, J. Minar, and V. Popescu, in *Band-Ferromagnetism*, Lecture Notes in Physics Vol. 580, edited by K. Baberschke, M. Donath, and W. Nolting (Springer-Verlag, Berlin, 2001), p. 371.
[20]G. E. Bacon and J. S. Plant, J. Phys. F **1**, 524 (1971).
[21]A. Coelho, TOPAS ACADEMIC, version 4.1 (2007).
[22]J. Kübler, *Theory of Itinerant Electron Magnetism* (Clarendon, Oxford, 2000).
[23]I. Galanakis, P. H. Dederichs, and N. Papanikolaou, Phys. Rev. B **66**, 174429 (2002).
[24]G. H. Fecher, H. C. Kandpal, S. Wurmehl, C. Felser, and G. Schönhense, J. Appl. Phys. **99**, 08J106 (2006).
[25]S. Wurmehl, H. C. Kandpal, G. H. Fecher, and C. Felser, J. Phys. Condens. Matter **18**, 6171 (2006).
[26]W. E. Pickett, Phys. Rev. B **57**, 10613 (1998).
[27]A. Dannenberg, M. Siewert, M. E. Gruner, M. Wuttig, and P. Entel, Phys. Rev. B **82**, 214421 (2010).